Research Square

Preprints are preliminary reports that have not undergone peer review.
They should not be considered conclusive, used to inform clinical practice,
or referenced by the media as validated information.

4-Octyl Itaconate promotes dendritic cell tolerogenic properties via suppressing STING signaling to delay lupus onset

Bo Zhu

zhubo@ujs.edu.cn

Jiangsu University

Lihua Zhu

Affiliated Hospital of Jiangsu University

Xue Wang

Affiliated Hospital of Jiangsu University

Luyao Yu

Affiliated Hospital of Jiangsu University

Zongxia Ge

Affiliated Hospital of Jiangsu University

Article

Keywords: Itaconate, systemic lupus erythematosus, tolerogenic dendritic cells, STING, Autoimmune diseases

Posted Date: June 5th, 2026

DOI: https://doi.org/10.21203/rs.3.rs-9575020/v1

License: This work is licensed under a Creative Commons Attribution 4.0 International License.
Read Full License

Additional Declarations: There is no conflict of interest

Abstract

Systemic lupus erythematosus (SLE) is a refractory autoimmune disease characterized by immune tolerance breakdown and dendritic cell (DCs) hyperactivation. Tolerogenic DCs (tolDCs) represent a promising therapeutic strategy, yet the regulatory mechanisms remain poorly understood. Here, we investigated the therapeutic potential and mechanism of the 4-octyl itaconate (4OI) and 4OI-induced tolDCs in SLE. In a chromatin-induced murine lupus model, 4OI administration significantly delayed disease onset, reduced proteinuria, anti-dsDNA autoantibodies, and renal pathological injury. Mechanistically, 4OI directly promoted a tolDCs phenotype both in vivo and in vitro, as evidenced by downregulated CD80/CD86, upregulated PD-L1, increased IL-10/TGF-β, and impaired $CD4^+$ T cell proliferation. Adoptive transfer of 4OI-induced tolDCs alleviated lupus progression, reducing Tfh, Th1, Th17, and plasma cells while increasing Tregs. Further investigation showed that 4OI promotes tolDCs differentiation by inhibiting STING transcription and phosphorylation. Notably, combining 4OI with the JAK inhibitor produced synergistic therapeutic effects superior to either monotherapy. These findings identify a previously unrecognized role of itaconate derivatives in promoting tolDCs via STING inhibition and suggest that 4OI and 4OI-induced tolDCs represents an attractive candidate for SLE therapy.

Introduction

Systemic lupus erythematosus (SLE) is a complex autoimmune disease characterized by excessive type I interferon production, abundant proinflammatory cytokines and autoantibodies, and widespread immune complex deposition[1,2]. Central to its pathogenesis is a breakdown in immune tolerance, which drives hyperactivation of both innate and adaptive immunity[3,4]. Innate sensing of self-antigens serves as the critical trigger that unleashes autoreactive immune responses. As the principal antigen-presenting cells, dendritic cells (DCs) bridge innate and adaptive immunity and, by orchestrating either tolerance or activation, shape SLE pathogenesis[5].

Substantial phenotypic and functional alterations of DCs have been reported in patients with SLE[6,7]. Although reduced in peripheral blood, DCs from these patients show increased infiltration into inflamed tissues and display an overactivated state, marked by upregulated co-stimulatory molecules (CD86, CD80) and enhanced secretion of proinflammatory cytokines (IL-12, IL-1β)[8]. These aberrantly activated DCs drive the differentiation of T follicular helper cells (Tfh) and Th17 cells[9–11], which in turn promotes B cell production of pathogenic autoantibodies and accelerates lupus progression. Conversely, tolDCs promote immune tolerance by inducing regulatory T(Treg) or B cells and suppressing conventional T and B cell activation, thereby preventing pathological inflammation and autoimmunity[12–14]. Therefore, blocking pathogenic DCs functions or restoring their tolerogenic capacity represents a particularly promising therapeutic strategy for SLE.

Recent studies have revealed that metabolic enzymes and metabolites play important roles in modulating DCs maturation and function[15]. Various metabolites have been found to either enhance or

inhibit DCs-mediated immune responses[16,17]. For example, the glycolytic metabolite NAD^+ promotes DCs migration by stabilizing F-actin polarization and polymerization[18]. Itaconate, a tricarboxylic acid (TCA) cycle metabolite, has recently gained increasing attention for its immunomodulatory properties[19–21]. It plays a crucial role in immune regulation by modulating signal transduction and post-translational modifications. Itaconate is generated by aconitate decarboxylase (ACOD1), the enzyme encoded by the immune-responsive gene IRG1. Several studies indicate that the ACOD1-itaconate pathway modulates immune dysregulation and associates with disease activity in SLE[22,23]. However, it remains unclear whether and how itaconate regulates the tolerogenic properties of DCs during lupus development.

In this study, we identify a previously unrecognized function of itaconate derivatives in promoting the tolerogenic properties of DCs during lupus development. STING signaling is a key mediator of innate immune activation and has been linked to autoimmunity; however, its regulation by itaconate in DCs remains unexplored. We further demonstrate that 4-octyl itaconate (4OI) promotes a tolDCs phenotype by inhibiting STING signaling and delays lupus onset. These findings suggest that 4OI and 4OI-induced tolDCs may represent a promising therapeutic strategy for SLE.

Results

Administration of 4OI alleviates disease onset and progression in lupus mice

To investigate the effects of 4OI on lupus onset and severity, we employed a chromatin-induced lupus mouse model. Mice received intraperitoneal injections of 4OI three times per week from weeks 3 to 6 post-immunization (Fig. 1a), and proteinuria was monitored dynamically. 4OI-treated mice exhibited significantly lower proteinuria levels than vehicle-treated controls between weeks 6 and 12 (Fig. 1b). To assess the impact of 4OI on renal function and inflammatory responses during disease progression, we measured serum creatinine (CREA), blood urea nitrogen (BUN), and anti-double-stranded DNA (dsDNA) autoantibodies at 4, 8 and 12 weeks after immunization. Renal pathology was evaluated at early (8 weeks) and late (12 weeks) stages of lupus nephritis by H&E staining, PAS staining and IgG immunofluorescence. Compared with vehicle-treated controls, 4OI treatment significantly reduced CREA, BUN and anti-dsDNA autoantibody levels at both disease stages (Fig. 1c–e). Morphologically, 4OI-treated mice showed marked improvement in renal histology, with substantially alleviated inflammation (Fig. 1f, H&E), attenuated glomerulosclerosis (Fig. 1f, PAS) and reduced immune complex deposition (Fig. 1f, IgG). Collectively, *in vivo* administration of 4OI delayed disease onset, ameliorated lupus nephritis and reduced circulating autoantibody levels in chromatin-induced lupus mice.

4OI drives the differentiation of tolDCs with tolerogenic phenotype in lupus mice

Tolerogenic dendritic cells (tolDCs) promote immune tolerance and suppress pathological inflammation and autoimmunity in SLE, thereby contributing to immune homeostasis during the early phase of

disease. To assess whether 4OI administration alters DCs phenotype and differentiation and delays disease onset in lupus mice, we analyzed the expression levels of phenotype-related molecules on $CD11c^+$ $MHCII^+$ DCs in the spleen (Fig. 2a) and draining inguinal lymph nodes (Fig. 2c) by flow cytometry. Immunostimulatory molecules on both splenic and lymph node DCs were markedly higher in 4OI-treated mice than in normal controls (Fig. 2b, d); however, relative to vehicle-treated controls, 4OI-treated mice exhibited significantly downregulated expression of these molecules and significantly upregulated expression of the immunosuppressive molecule PD-L1 (Fig. 2b, d). These findings suggest that 4OI administration may drive DCs toward a tolerogenic phenotype *in vivo*.

To investigate whether 4OI acts directly on DCs, we added 4OI on days 5 and 7 during the *in vitro* differentiation of bone marrow-derived DCs (BMDCs) and extended the culture period to day 9 (Fig. 2e). We then assessed phenotypic changes, cytokine production, and the functional capacity of 4OI-treated DCs (4OI-DCs) to induce $CD4^+$ T cell proliferation, thereby testing whether 4OI drives DCs differentiation toward a tolerogenic phenotype. 4OI-DCs expressed substantially lower levels of CD80 and CD86 than untreated controls (DCs), whereas expression of PD-L1 and the immunosuppressive cytokines IL-10 and TGF-β was significantly increased (Fig. 2g, h). Concordantly, 4OI-DCs showed a markedly reduced capacity to induce $CD4^+$ T cell proliferation (Fig. 2f). Together, these findings demonstrate that 4OI directly drives DCs differentiation toward a tolerogenic phenotype.

Adoptive transfer of 4OI-induced tolDCs effectively alleviates the progression of lupus.

To determine whether 4OI-induced tolDCs exert immunosuppressive functions *in vivo*, we adoptively transferred either DCs or 4OI-induced tolDCs into chromatin-induced lupus mice (Fig. 3a). Compared with both lupus control mice and recipients of DCs, mice that received 4OI-induced tolDCs exhibited a marked amelioration of disease severity, as reflected by significantly reduced serum levels of anti-dsDNA autoantibodies, CREA and BUN, as well as decreased urinary protein (Fig. 3b). These improvements were accompanied by attenuated glomerular damage and reduced immune complex deposition in the kidneys (Fig. 3c, d). Moreover, the frequencies and absolute numbers of Tfh cells, plasma cells, Th1 cells and Th17 cells in the spleens and lymph nodes were profoundly decreased (Fig. 3e-g). Collectively, these findings demonstrate that 4OI-induced tolDCs possess potent immunosuppressive activity and hold therapeutic potential for the treatment of lupus-prone mice.

4OI promotes a tolerogenic DCs phenotype by inhibiting STING transcription and phosphorylation

To understand the mechanism by which 4OI regulates tolDCs differentiation, we performed RNA sequencing using the DCs freshly isolated from the spleen of 4OI-treated and control lupus mice. Intriguingly, the expression of IFN-β and a large subset of IFN-responsive genes were reduced in the DCs from the spleen of 4OI-treated lupus mice (Fig. 4a). Our RNA sequencing data also revealed that the administration of 4OI inhibited the expression of several cytokines, including Il-6, Il-12a and Il-12b (Fig. 4a). The expression of genes associated with DCs maturation was also downregulated in 4OI-treated DCs (Fig. 4a). Additionally, gene set enrichment analysis (GSEA) revealed that the enrichment of

the interferon response, particularly the interferon alpha response, was attenuated in 4OI-treated DCs (Fig. 4b). We further validated the RNA sequencing results by qRT-PCR, and IFN-β and IFN-α4 tested were found to be downregulated in the DCs from the spleen of 4OI-treated lupus mice (Fig. 4c). Furthermore, upon ALD-DNA stimulation, 4OI treatment in DCs suppressed the induction of type I interferons (Fig. 4d). These data suggest that 4OI treatment in DCs inhibits the ALD-DNA-triggered induction of type I IFNs and IFN-responsive genes.

The findings that the induction of type I IFNs was significantly abrogated in the 4OI-treated DCs indicated that 4OI might be affected in cytosolic DNA sensing in DCs. As expected, the expression of cytosolic DNA sensing-associated genes in DCs from the spleens of 4OI-treated lupus mice was markedly dysregulated (Fig. 4f). To confirm the role of 4OI in cytosolic DNA sensing, we transfected purified herring testes DNA (HT-DNA) which mimics ALD-DNA, to stimulate the cytoplasmic DNA-sensing pathways in DCs. Indeed, the 4OI treatment inhibits cytosolic DNA-triggered phosphorylation of IRF3 and TBK1 (Fig. 4g). Previous reports have shown that 4OI alkylates STING and blocks its phosphorylation[24,25]. Here, to assess the impact of 4OI on STING phosphorylation, we stimulated DCs with 2',3'-cGAMP to activate the cGAS-STING pathway. Treatment with 4OI resulted in a marked, dose-dependent reduction of STING phosphorylation (Fig. 4h). To test whether 4OI-induced DCs tolerance depends on suppression of STING phosphorylation, we co-treated DCs with DMXAA, a STING agonist, aiming to reverse 4OI-mediated blockade of STING activation. Of note, DMXAA only partially reversed the effects of 4OI on DC functions, including IL-10 expression, surface levels of CD80, CD86 and PD-L1, as well as the ability of DCs to restrain T cell proliferation (Fig. 4i-k). Collectively, these data indicate that 4OI-induced DCs tolerance is mediated, at least in part, through inhibition of STING phosphorylation.

The transcription factor NRF2 is a key downstream target of itaconate and critically maintains the tolerogenic state of DCs[26,27]. NRF2 has been shown to suppress STING expression by reducing STING mRNA stability[28]. In our study, treatment of DCs with 4OI for 24 hours led to a marked increase in NRF2 protein levels and a concomitant decrease in STING protein abundance, suggesting that 4OI may downregulate STING expression via NRF2 (Fig. 4l). Moreover, 4OI reduced STING mRNA levels, and this effect was reversed upon NRF2 knockdown (Fig. 4m). Together, these data indicate that the NRF2-STING axis may also mediate 4OI-induced DC tolerance.

4OI synergize with JAK inhibitor in the treatment of Lupus.

An increasing number of studies have reported STING-dependent mechanisms beyond the canonical type I interferon (IFN-I) pathway. To investigate whether 4OI ameliorates lupus pathogenesis via the STING-IFN-I axis, we used baricitinib, a selective Janus kinase (JAK)1/2 inhibitor targeting the IFNAR1 pathway that has shown therapeutic efficacy in clinical trials of SLE, as a positive control. We further explored the therapeutic effect of combining 4OI with baricitinib in lupus treatment. Notably, although monotherapy with either compound alleviated disease manifestations to some extent, their combination produced a markedly enhanced therapeutic effect (Fig. 5a-c), suggesting a synergistic interaction between 4OI and baricitinib. Compared with either 4OI or baricitinib monotherapy, the combination of 4OI

and baricitinib significantly reduced serum levels of anti-dsDNA antibodies, improved renal function (Fig. 5b), and attenuated glomerular injury as well as renal immune complex deposition (Fig. 5c). As expected, splenic DCs from mice treated with the combination exhibited a tolerogenic phenotype, characterized by markedly reduced expression of the costimulatory molecules CD80 and CD86 and a pronounced upregulation of PD-L1 (Fig. 5d). Further phenotypic analysis revealed that combination therapy substantially increased the frequency of splenic Treg cells (Fig. 5f), whereas PCs, Tfh cells, and Th17 cells remained largely unaffected (Fig. 5e). Collectively, these findings highlight the critical roles of 4OI and STING in regulating DCs-mediated autoimmunity and lupus progression, and suggest that co-targeting the itaconate pathway and IFN-I signaling may represent a promising strategy to enhance therapeutic efficacy and induce disease remission.

Discussion

In this study, we demonstrated that administration of 4OI to lupus mice delayed disease onset and ameliorated lupus-like symptoms. Mechanistically, 4OI promoted the differentiation of tolDCs through suppression of STING signaling. Furthermore, adoptive transfer of 4OI-induced tolDCs alleviated lupus progression, reducing Tfh, Th1, Th17, and plasma cells while increasing Tregs. Notably, combination of 4OI with a JAK inhibitor produced synergistic therapeutic effects superior to either agent alone. Collectively, these results suggest that 4OI and 4OI-induced tolDCs represents a promising candidate for the treatment of SLE.

Extensive evidence indicates that itaconate, an intermediate metabolite of the tricarboxylic acid cycle, plays important roles in anti-inflammatory and anti-oxidative stress responses[29]. Recent studies have established that itaconate also plays key roles in immunometabolism, mediating important immunomodulatory functions [30]. Notably, emerging research has shown that itaconate levels are significantly reduced in the serum of patients with lupus complicated by cardiovascular disease, and that its reduction is closely associated with cardiovascular disease markers and disease activity[23]. In a TLR7-induced lupus mouse model, genetic ablation of the endogenous itaconate-producing gene ACOD1 exacerbated lupus nephritis and enhanced the activation of inflammatory immune cells, including macrophages and neutrophils[23]. Conversely, administration of itaconate to lupus-prone mice abrogated immune dysregulation and clinical features[22]. Together, these findings suggest that the endogenous itaconate pathway is involved in lupus pathogenesis and is closely linked to immune dysregulation in lupus. However, further investigations are needed to characterize the roles of itaconate in immune cell differentiation/function and the maintenance of immune tolerance during lupus pathogenesis.

Blanco et al. reported that administration of 4OI to genetically deficient lupus-prone mice after clinical disease onset exerted therapeutic effects in established lupus. In our study, using a chromatin-induced lupus mouse model, we administered 4OI during early disease development and found that it delayed lupus onset. Moreover, DCs in the spleen and lymph nodes of 4OI-treated lupus mice displayed a tolerogenic phenotype. Using the chromatin-induced lupus model, we further demonstrated that 4OI

sustains immune tolerance by promoting tolerogenic DCs differentiation. However, whether similar effects occur in other lupus models, such as TLR7-induced lupus or conventional lupus-prone mice, remains to be determined.

In recent years, accumulating evidence has established that tolDCs are critical for maintaining immune tolerance and preventing autoimmune diseases[12–14]. TolDCs enforce immunological tolerance through multiple mechanisms, including the induction of T cell unresponsiveness, the generation of Treg cells, the suppression of T cell responses, and the promotion of T cell apoptosis[13]. However, the network of environmental signals and cell-intrinsic programs that govern tolDCs remains poorly understood. Several studies have implicated tissue microenvironment-derived factors in modulating tolDCs function. For example, intestinal epithelial cell-derived cytokines such as TSLP, retinoic acid, vitamin C/D3, TGF-β, and IL-25 instruct DCs to acquire a tolerogenic phenotype, characterized by reduced IL-12 and IL-23 production and increased IL-10 secretion, which in turn curtails Th1 responses and fosters Treg cell generation[31–34]. Recent work has further revealed that metabolic enzymes and metabolites contribute to the pathogenesis of autoimmune diseases by shaping DCs function and migration[35]. These include the regulation of DCs tolerogenicity via succinylation[36], the promotion of DCs migration through mitochondrial dynamics[37], and the control of chemokine-driven DCs trafficking[38]. Nevertheless, whether metabolites such as itaconate are involved in regulating tolDCs differentiation remains largely unexplored. Our previous study showed that itaconate in the tumor microenvironment suppresses DCs maturation and compromises DCs-mediated antitumor immunity[16]. In the present study, we demonstrate that the itaconate derivative 4OI promotes tolDCs differentiation, induces immune tolerance, and delays lupus onset.

The pathogenic consequences of aberrant nucleic acid sensing are clearly manifested in SLE[39,40], where clinically elevated cGAMP and robust monocytic STING expression render patient serum sufficient to trigger robust IFN-I responses[41,42]. Preclinical models, such as IMQ-induced lupus mice, corroborate that STING exacerbates disease partially by shaping a proinflammatory[43]. Addressing this pathogenic mechanism, our findings demonstrate that 4OI administration limits chromatin-induced murine lupus by reprogramming DCs towards a tolerogenic state. However, the spatiotemporal dynamics of STING expression and activation during pathogenesis, and whether STING directly dictates tolDCs differentiation, remain elusive. Mechanistically, our findings align with previous reports indicating that 4OI represses STING transcription via NRF2 activation[28]. While NRF2 is a well-characterized target of 4OI and critical for tolDCs maintenance, the capacity of 4OI to actively induce tolDCs differentiation has not been previously described. Future studies employing Irg1- and Sting-knockout models are warranted to delineate the cell-intrinsic roles of endogenous itaconate and STING in orchestrating tolDCs differentiation and functional stability.

Collectively, our study uncovers a previously unappreciated role for 4OI in enforcing DCs tolerance, which sequentially restrains pathogenic adaptive immunity and delays lupus onset. Consequently, the

pharmacological administration of 4OI, or the adoptive transfer of 4OI-induced tolDCs, emerges as a highly promising therapeutic strategy for the treatment of SLE.

Materials and methods

Animals

Female C57BL/6 mice were purchased from the Laboratory Animal Research Center at the Jiangsu University. OT-II mice were obtained from The Jackson Laboratory. Mice were maintained in the Laboratory Animal Research Center of Jiangsu University (Jiangsu, China). All the animal experimental procedures were approved by the Animal Care and Use Committee of Jiangsu University (No: UJS-IACUC-AP-2023022803). Animals were kept under the Specific Pathogen Free (SPF) environment with 12/12 h dark/light cycles at 26 ± 1°C. All animal procedures were conducted in accordance with the National Institutes of Health Guide for the Care and Use of Laboratory Animals (NIH Publication No. 85–23, revised 1996).

Establishment of chromatin-induced lupus mouse model

To establish a chromatin-induced lupus mouse model[44,45], chromatin extracted from apoptotic splenocytes was used as the antigen for subcutaneous immunization in 8-week-old female C57BL/6 mice. Briefly, nuclear chromatin was isolated from splenocytes stimulated with 5 ng/mL concanavalin A (ConA; Sigma-Aldrich) for 72 h. On day 0, mice were subcutaneously immunized with 200 μg of chromatin emulsified in complete Freund's adjuvant (CFA, InvivoGen). Booster immunizations were administered on day 14 and 28 using 200 μg of chromatin emulsified in incomplete Freund's adjuvant (IFA, InvivoGen).

For 4OI and baricitinib treatment, female C57BL/6 mice were immunized subcutaneously with chromatin/CFA on day 0, and mice were boosted with chromatin /IFA on day 14 and day 28. From the first day of the third week of the first immunization, mice were intraperitoneally injected with of 4OI (25mg/kg) (MedChemExpress) and baricitinib (5mg/kg) (MedChemExpress) or Vehicle control three times weekly for four weeks.

Serologic analysis and urinalysis

Serum samples were collected from lupus mice for the measurement of anti-double-stranded DNA (anti-dsDNA) antibodies, urea, and creatinine. Anti-dsDNA antibody levels were measured using a mouse anti-dsDNA ELISA kit (CUSABIO), whereas urea and creatinine levels were determined using a Urea Assay Kit and a Creatinine Assay Kit, respectively (Nanjing Jiancheng Bioengineering Institute). Urinary protein concentrations were assessed using 10SG Urine Reagent Strips (URIT).

Histological assessment

Kidney tissues from lupus mice were fixed in 4% paraformaldehyde, embedded in paraffin, and sectioned for histological analysis. Sections were stained with hematoxylin and eosin (H&E) or periodic acid-Schiff (PAS) according to standard protocols and imaged using a high-resolution light microscope (Olympus).

Immunofluorescence

Mouse kidneys were embedded in OCT compound and cryosectioned to 10 μm-thick sections. Sections were fixed in 4% paraformaldehyde for 15 minutes, washed with PBS, and blocked with 5% bovine serum albumin (BSA) at room temperature for 1 hour. Sections were incubated with a primary anti-mouse IgG antibody at 4°C overnight, followed by incubation with a fluorophore-conjugated secondary antibody at room temperature for 30 minutes. After three washes with PBS-T (PBS containing .3% Triton X-100), nuclei were counterstained with 4',6-diamidino-2-phenylindole (DAPI, Biosharp) for 5 minutes. Sections were mounted with fluorescence mounting medium. Images were acquired on a Carl Zeiss LSM800 fluorescence microscope.

BMDCs culture

BMDCs were generated as described previously[16]. Briefly, bone marrow cells isolated from 8-week-old C57BL/6 mice were seeded at a density of 1×10^6 cells per well in a 24-well plate in RPMI-1640 supplemented with 10% FBS, penicillin-streptomycin (100 U/mL), GM-CSF (20 ng/mL, PeproTech), and IL-4 (5 ng/mL, PeproTech). An equal volume of fresh complete medium was added on days 3 and 5. On day 7, non-adherent cells were collected.

Dendritic cell and $CD4^+$ naïve T-cell coculture

$CD4^+$ T cells were enriched from the spleens of OT-II mice by magnetic separation using the Dynal mouse CD4-negative selection kit (BioLegend). The sorted $CD4^+$ T cells were labeled with CFSE (eBioscience) at 37°C for 10 minutes, washed, and counted prior to co-culture with BMDCs. A total of 5×10^4 BMDCs were incubated with either endotoxin-free ovalbumin (OVA) protein (50 μg/mL, InvivoGen) or the $OVA_{323-339}$ peptide (5 μg/mL, MedChemExpress) for 5 hours in 96-well plates. After incubation, the BMDCs were washed and co-cultured with 1×10^5 OT-II T cells. T cell proliferation was assessed by flow cytometry after 72 hours of co-culture.

Flow cytometry

Spleens and draining inguinal lymph nodes were isolated from mice, and single-cell suspensions were prepared in culture medium. Surface/intracellular markers were detected by using the following monoclonal antibodies: anti-mouse CD11c(N418), MHC-II(NIMR-4), CD80(16-10A1), CD86(GL1), CD4(RM4-5), CXCR5(SPRCL5), PD1(RMP1-30), CD138(300506), B220(RA3-6B2), IL-17A(eBio17B7), IFN-γ(XMG1.2) antibodies were purchased from eBioscience. Anti-mouse PD-L1(10F.9G2), FOXP3(MF-14)

antibodies were purchased from BioLegend. For intracellular IL-17A and IFN-γ staining in $CD4^+$ T cells, isolated mouse splenocytes or inguinal lymph nodes cells were stimulated with Cell Stimulation Cocktail(eBioscience) for 5 hours at 37°C with 5% CO2. According to the intracellular staining Fixation/ Permeabilization Buffer (Invitrogen) procedure, cells were stained with antibodies for surface markers, fixed, permeabilized, and then stained with anti-mouse IFN-γ and IL-17A mAb. Intranuclear staining was performed using antibodies according to the Foxp3 Staining Buffer Set (eBioscience) protocol. Flow cytometry was performed on a BD FACSCanto II cytometer (BD Biosciences), and data were analyzed using FlowJo software (FlowJo, LLC).

Immunoblot analysis

Cells were lysed using RIPA lysis buffer supplemented with protease and phosphatase inhibitors. Protein lysates were separated by SDS-PAGE and transferred onto nitrocellulose membranes. Membranes were blocked with 5% bovine serum albumin (BSA) in PBST and then incubated overnight at 4°C with primary antibodies anti-mouse TBK1(3504S, Cell Signaling Technology), p-TBK1(5483s, Cell Signaling Technology), IRF3(66670-1-Ig, Proteintech), p-IRF3(4947, Cell Signaling Technology), STING(19851-1-AP, Proteintech), p-STING(72971, Cell Signaling Technology), GAPDH(sc-365062, Santa Cruz), NRF2 (12721, Cell Signaling Technology) and beta Tubulin(GB15140, Servicebio). Following primary antibody incubation, membranes were incubated with the appropriate secondary antibody for 2 hours at room temperature. Immunoreactive bands were detected using an ECL Western Blotting Substrate, and images were acquired using a chemiluminescence imaging system.

ALD-DNA preparation

Activated lymphocyte-derived DNA(ALD-DNA) was isolated as we previously described[46], splenocytes were stimulated with 5 ng/mL ConA (Sigma-Aldrich) for 72 hours. Genomic DNA from apoptotic splenocytes was treated with S1 nuclease (Thermo Scientific) and proteinase K (Sigma-Aldrich), then purified using DNeasy Blood & Tissue Kits (QIAGEN) following the manufacturer's instructions. This preparation was designated ALD-DNA.

ELISA

IFN-β concentrations in culture supernatants were quantified using a mouse IFN-β ELISA Set (EK2236, Lianke Biotechnology) according to the manufacturer's protocol.

siRNA interference

siRNA against mouse Nfe2l2 was purchased from Thermo Fisher (s70535). Oligonucleotide transfection was performed with Lipofectamine RNAiMAX Transfection Reagent (Invitrogen) according to the manufacturer's instructions.

RT-qPCR and RNA-seq analysis

Total RNA was extracted from cells lysed with TRIzol (Invitrogen). cDNA was synthesized from total RNA using HiScript III Reverse Transcriptase (Vazyme, R323-01) according to the manufacturer's protocol.

Gene transcripts were quantified by real-time quantitative PCR using ChamQ SYBR qPCR Master Mix (Vazyme, Q711-02). Primer sequences are provided in Supplemental Table 1. For RNA-seq analysis, total RNA was isolated from mouse spleen $CD11c^+$ cells with TRIzol (Invitrogen) and sequenced on an Illumina HiSeq or NovaSeq 2×150 platform by AZENTA Life Sciences (Suzhou). Differentially expressed genes were identified using edgeR with a fold-change cutoff of ≥ 2 and a p-value < 0.05. GO database were used to extrapolate differentially expressed pathways. RNA-seq data generated in this study are available upon request.

Statistical analysis

Statistical analyses were performed using GraphPad Prism 9 (GraphPad Software, Inc). Statistical comparisons were performed using the student's t-test or One-way ANOVA. Results are presented as mean ± SD. $P < 0.05$ was considered statistically significant.

Declarations

Data Availability Statement

Datasets analyzed in this study are available upon reasonable request to the corresponding author.

Funding Statement

This work was supported by the National Natural Science Foundation of China (No. 82302039), Open Project of Anhui Provincial Key Laboratory of Tumor Evolution and Intelligent Diagnosis and Treatment (No. KFKT202407).

Conflict of Interest

The authors declare no competing interests.

Ethics Statement

All animal experiments were approved by the Animal Care and Use Committee of Jiangsu University (No. UJS-IACUC-AP-2023022803) and were conducted in accordance with the US National Institutes of Health Guide for the Care and Use of Laboratory Animals (NIH Publication no. 85-23, revised 1996).

Author contributions

B.Z. conceived the project and designed the experiments. L.H.Z. and B.Z. wrote the paper. L.H.Z., X.W., L.Y.Y. performed the experiments and analyzed the data. Z.X.G. analyzed the data. B.Z. reviewed and edited the manuscript. All authors have read and approved the manuscript.

References

1. Kaul, A. *et al.* Systemic lupus erythematosus. *Nat Rev Dis Primers* **2**, 16039 (2016). https://doi.org:10.1038/nrdp.2016.39
2. Durcan, L., O'Dwyer, T. & Petri, M. Management strategies and future directions for systemic lupus erythematosus in adults. *Lancet* **393**, 2332-2343 (2019). https://doi.org:10.1016/S0140-6736(19)30237-5
3. Arnaud, L., Chasset, F. & Martin, T. Immunopathogenesis of systemic lupus erythematosus: An update. *Autoimmun Rev* **23**, 103648 (2024). https://doi.org:10.1016/j.autrev.2024.103648
4. Liang, Y. N. *et al.* Immune cells in systemic lupus erythematosus: biology and traditional Chinese medicine therapy. *Acta Pharmacol Sin* **46**, 2587-2596 (2025). https://doi.org:10.1038/s41401-025-01554-2
5. Liu, J., Zhang, X. & Cao, X. Dendritic cells in systemic lupus erythematosus: From pathogenesis to therapeutic applications. *J Autoimmun* **132**, 102856 (2022). https://doi.org:10.1016/j.jaut.2022.102856
6. Gerl, V. *et al.* Blood dendritic cells in systemic lupus erythematosus exhibit altered activation state and chemokine receptor function. *Ann Rheum Dis* **69**, 1370-1377 (2010). https://doi.org:10.1136/ard.2009.111021
7. Ding, D., Mehta, H., McCune, W. J. & Kaplan, M. J. Aberrant phenotype and function of myeloid dendritic cells in systemic lupus erythematosus. *J Immunol* **177**, 5878-5889 (2006). https://doi.org:10.4049/jimmunol.177.9.5878
8. Crispin, J. C., Vargas-Rojas, M. I., Monsivais-Urenda, A. & Alcocer-Varela, J. Phenotype and function of dendritic cells of patients with systemic lupus erythematosus. *Clin Immunol* **143**, 45-50 (2012). https://doi.org:10.1016/j.clim.2011.12.004
9. Yin, X., Chen, S. & Eisenbarth, S. C. Dendritic Cell Regulation of T Helper Cells. *Annu Rev Immunol* **39**, 759-790 (2021). https://doi.org:10.1146/annurev-immunol-101819-025146
10. Yao, C. *et al.* Skin dendritic cells induce follicular helper T cells and protective humoral immune responses. *J Allergy Clin Immunol* **136**, 1387-1397 e1381-1387 (2015). https://doi.org:10.1016/j.jaci.2015.04.001
11. Hilligan, K. L. & Ronchese, F. Antigen presentation by dendritic cells and their instruction of CD4+ T helper cell responses. *Cell Mol Immunol* **17**, 587-599 (2020). https://doi.org:10.1038/s41423-020-0465-0
12. Morante-Palacios, O., Fondelli, F., Ballestar, E. & Martinez-Caceres, E. M. Tolerogenic Dendritic Cells in Autoimmunity and Inflammatory Diseases. *Trends Immunol* **42**, 59-75 (2021). https://doi.org:10.1016/j.it.2020.11.001
13. Liu, J. & Cao, X. Regulatory dendritic cells in autoimmunity: A comprehensive review. *J Autoimmun* **63**, 1-12 (2015). https://doi.org:10.1016/j.jaut.2015.07.011
14. Adams, N. M. *et al.* Transcription factor Etv3 controls the tolerogenic function of dendritic cells. *Science* **391**, eads1246 (2026). https://doi.org:10.1126/science.ads1246

15. Chen, J., Liu, J. & Cao, X. Functional and Metabolic Heterogeneity of Dendritic Cells in Self-Tolerance and Autoimmunity. *Immunol Rev* **336**, e70068 (2025). https://doi.org:10.1111/imr.70068
16. Zhu, B. *et al.* 4-Octyl Itaconate Modulates Dendritic Cells Function and Tumor Immunity via NRF2 Activation. *J Inflamm Res* **18**, 5699-5713 (2025). https://doi.org:10.2147/JIR.S516085
17. Sanmarco, L. M. *et al.* Lactate limits CNS autoimmunity by stabilizing HIF-1alpha in dendritic cells. *Nature* **620**, 881-889 (2023). https://doi.org:10.1038/s41586-023-06409-6
18. Liu, J. *et al.* CCR7 Chemokine Receptor-Inducible lnc-Dpf3 Restrains Dendritic Cell Migration by Inhibiting HIF-1alpha-Mediated Glycolysis. *Immunity* **50**, 600-615 e615 (2019). https://doi.org:10.1016/j.immuni.2019.01.021
19. Liu, Y. *et al.* Itaconate: A key regulator of immune responses and potential therapeutic target for autoimmune and inflammatory diseases. *Autoimmun Rev* **24**, 103885 (2025). https://doi.org:10.1016/j.autrev.2025.103885
20. Aso, K. *et al.* Itaconate ameliorates autoimmunity by modulating T cell imbalance via metabolic and epigenetic reprogramming. *Nat Commun* **14**, 984 (2023). https://doi.org:10.1038/s41467-023-36594-x
21. Hooftman, A. & O'Neill, L. A. J. The Immunomodulatory Potential of the Metabolite Itaconate. *Trends Immunol* **40**, 687-698 (2019). https://doi.org:10.1016/j.it.2019.05.007
22. Blanco, L. P. *et al.* Modulation of the Itaconate Pathway Attenuates Murine Lupus. *Arthritis Rheumatol* **74**, 1971-1983 (2022). https://doi.org:10.1002/art.42284
23. Patino-Martinez, E. *et al.* The Aconitate Decarboxylase 1/Itaconate Pathway Modulates Immune Dysregulation and Associates with Cardiovascular Disease Markers and Disease Activity in Systemic Lupus Erythematosus. *J Immunol* **213**, 419-434 (2024). https://doi.org:10.4049/jimmunol.2400241
24. Su, C., Cheng, T., Huang, J., Zhang, T. & Yin, H. 4-Octyl itaconate restricts STING activation by blocking its palmitoylation. *Cell Rep* **42**, 113040 (2023). https://doi.org:10.1016/j.celrep.2023.113040
25. Li, W. *et al.* 4-octyl itaconate as a metabolite derivative inhibits inflammation via alkylation of STING. *Cell Rep* **42**, 112145 (2023). https://doi.org:10.1016/j.celrep.2023.112145
26. Mills, E. L. *et al.* Itaconate is an anti-inflammatory metabolite that activates Nrf2 via alkylation of KEAP1. *Nature* **556**, 113-117 (2018). https://doi.org:10.1038/nature25986
27. Wei, H. J. *et al.* Nrf2-mediated metabolic reprogramming of tolerogenic dendritic cells is protective against aplastic anemia. *J Autoimmun* **94**, 33-44 (2018). https://doi.org:10.1016/j.jaut.2018.07.005
28. Olagnier, D. *et al.* Nrf2 negatively regulates STING indicating a link between antiviral sensing and metabolic reprogramming. *Nat Commun* **9**, 3506 (2018). https://doi.org:10.1038/s41467-018-05861-7
29. Peace, C. G. & O'Neill, L. A. The role of itaconate in host defense and inflammation. *J Clin Invest* **132** (2022). https://doi.org:10.1172/JCI148548

30. McGettrick, A. F., Bourner, L. A., Dorsey, F. C. & O'Neill, L. A. J. Metabolic Messengers: itaconate. *Nat Metab* **6**, 1661-1667 (2024). https://doi.org:10.1038/s42255-024-01092-x
31. Lu, M. *et al.* Homeostatic maturation programs drive human cDC2s into a tolerogenic state. *Immunity* (2026). https://doi.org:10.1016/j.immuni.2026.01.028
32. Castenmiller, C., Keumatio-Doungtsop, B. C., van Ree, R., de Jong, E. C. & van Kooyk, Y. Tolerogenic Immunotherapy: Targeting DC Surface Receptors to Induce Antigen-Specific Tolerance. *Front Immunol* **12**, 643240 (2021). https://doi.org:10.3389/fimmu.2021.643240
33. Morante-Palacios, O. *et al.* Vitamin C enhances NF-kappaB-driven epigenomic reprogramming and boosts the immunogenic properties of dendritic cells. *Nucleic Acids Res* **50**, 10981-10994 (2022). https://doi.org:10.1093/nar/gkac941
34. Nagy, N. A. *et al.* Retinoic acid-loaded liposomes induce human mucosal CD103(+) dendritic cells that inhibit Th17 cells and drive regulatory T-cell development in vitro. *Eur J Immunol* **54**, e2350839 (2024). https://doi.org:10.1002/eji.202350839
35. Patino-Martinez, E. & Kaplan, M. J. Immunometabolism in systemic lupus erythematosus. *Nat Rev Rheumatol* **21**, 377-395 (2025). https://doi.org:10.1038/s41584-025-01267-0
36. Zhang, X. *et al.* Metabolic enzyme Suclg2 maintains tolerogenicity of regulatory dendritic cells diffDCs by suppressing Lactb succinylation. *J Autoimmun* **138**, 103048 (2023). https://doi.org:10.1016/j.jaut.2023.103048
37. Zhang, X. *et al.* Farnesyl pyrophosphate potentiates dendritic cell migration in autoimmunity through mitochondrial remodelling. *Nat Metab* **6**, 2118-2137 (2024). https://doi.org:10.1038/s42255-024-01149-x
38. Liu, J. *et al.* Glycosyltransferase Extl1 promotes CCR7-mediated dendritic cell migration to restrain infection and autoimmunity. *Cell Rep* **42**, 111991 (2023). https://doi.org:10.1016/j.celrep.2023.111991
39. Crowl, J. T., Gray, E. E., Pestal, K., Volkman, H. E. & Stetson, D. B. Intracellular Nucleic Acid Detection in Autoimmunity. *Annu Rev Immunol* **35**, 313-336 (2017). https://doi.org:10.1146/annurev-immunol-051116-052331
40. Wang, M. M. *et al.* The role of the cGAS-STING signaling pathway in viral infections, inflammatory and autoimmune diseases. *Acta Pharmacol Sin* **45**, 1997-2010 (2024). https://doi.org:10.1038/s41401-023-01185-5
41. Kato, Y. *et al.* Apoptosis-derived membrane vesicles drive the cGAS-STING pathway and enhance type I IFN production in systemic lupus erythematosus. *Ann Rheum Dis* **77**, 1507-1515 (2018). https://doi.org:10.1136/annrheumdis-2018-212988
42. Murayama, G. *et al.* Inhibition of mTOR suppresses IFNalpha production and the STING pathway in monocytes from systemic lupus erythematosus patients. *Rheumatology (Oxford)* **59**, 2992-3002 (2020). https://doi.org:10.1093/rheumatology/keaa060
43. Liu, Y. *et al.* Role of STING Deficiency in Amelioration of Mouse Models of Lupus and Atherosclerosis. *Arthritis Rheumatol* **77**, 547-559 (2025). https://doi.org:10.1002/art.43062

44. Ma, K. *et al.* TLR4(+)CXCR4(+) plasma cells drive nephritis development in systemic lupus erythematosus. *Ann Rheum Dis* **77**, 1498-1506 (2018). https://doi.org:10.1136/annrheumdis-2018-213615

45. Ma, K. *et al.* IL-17 sustains the plasma cell response via p38-mediated Bcl-xL RNA stability in lupus pathogenesis. *Cell Mol Immunol* **18**, 1739-1750 (2021). https://doi.org:10.1038/s41423-020-00540-4

46. Rui, K. *et al.* Myeloid-Derived Suppressor Cell-Derived Interferon-beta Promotes T Follicular Helper Cell Response and Exacerbates Lupus Development. *Arthritis Rheumatol* (2025). https://doi.org:10.1002/art.70004

Figures

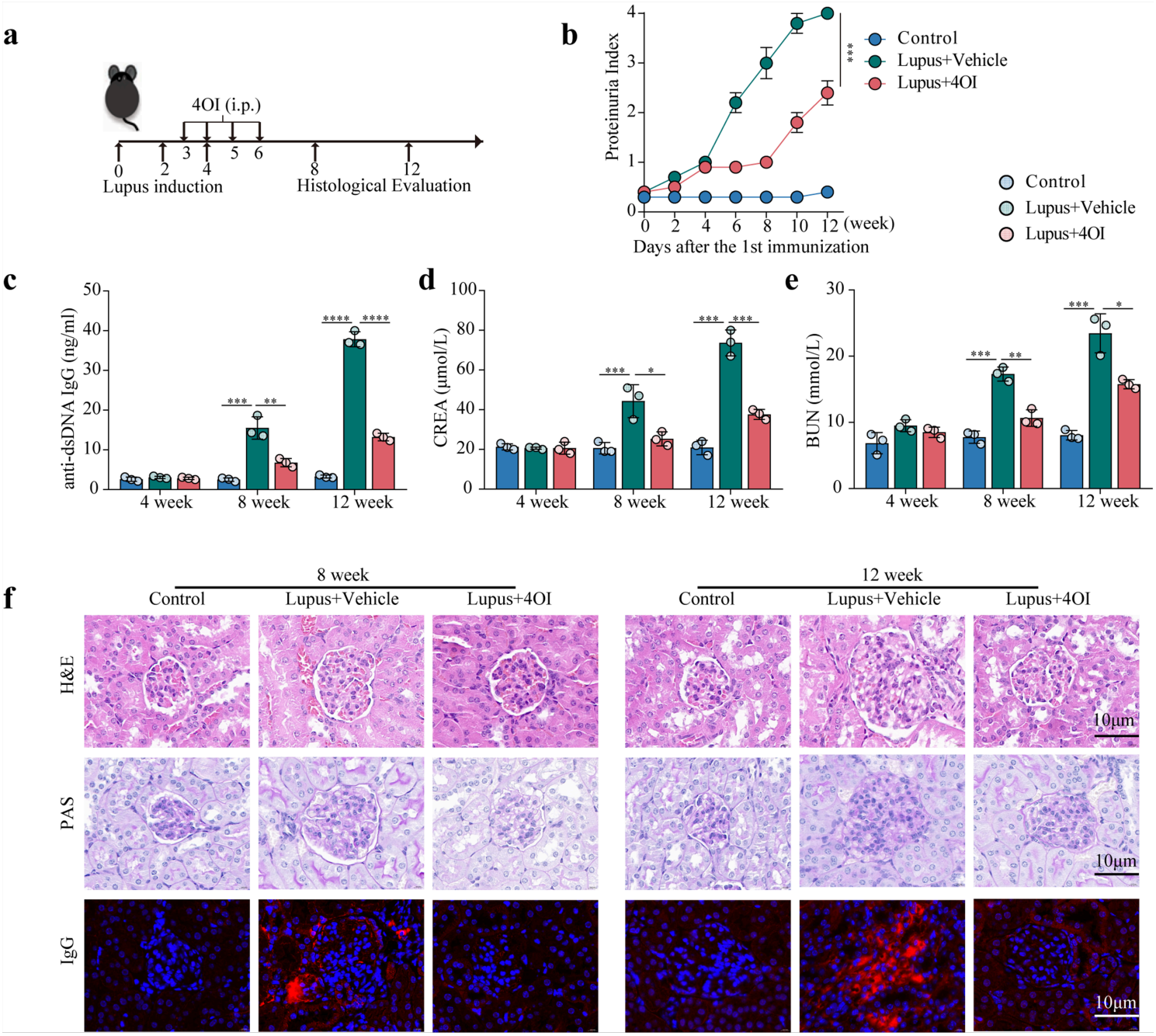


Figure 1

4OI alleviate disease onset and progression in lupus mice. (a) A graphic scheme of lupus induction and 4OI administration. Eight-week-old female C57BL/6 mice were immunized subcutaneously with chromatin/CFA on week 0, and mice were boosted with chromatin/IFA on weeks 2 and 4. From the first day of the third week of the first immunization, mice were intraperitoneally injected with 4OI or Vehicle for four weeks. Mice were sacrificed on week 8 and 12 (n = 3 per group). (b) The protein levels in the urine from different groups were monitored every two weeks. Concentrations of serum anti-dsDNA IgG(c), creatinine(d), and urea(e) were measured at weeks 4, 8, and 12 after the initial immunization in different groups. (f) Representative images show kidney sections stained with H&E, PAS staining, and IgG immunofluorescence staining. Scale bar =10μm. The data were obtained from at least three independent experiments. (means ± SDs; **** $p < 0.0001$; *** $p < 0.001$; ** $p < 0.01$; * $p < 0.05$.)

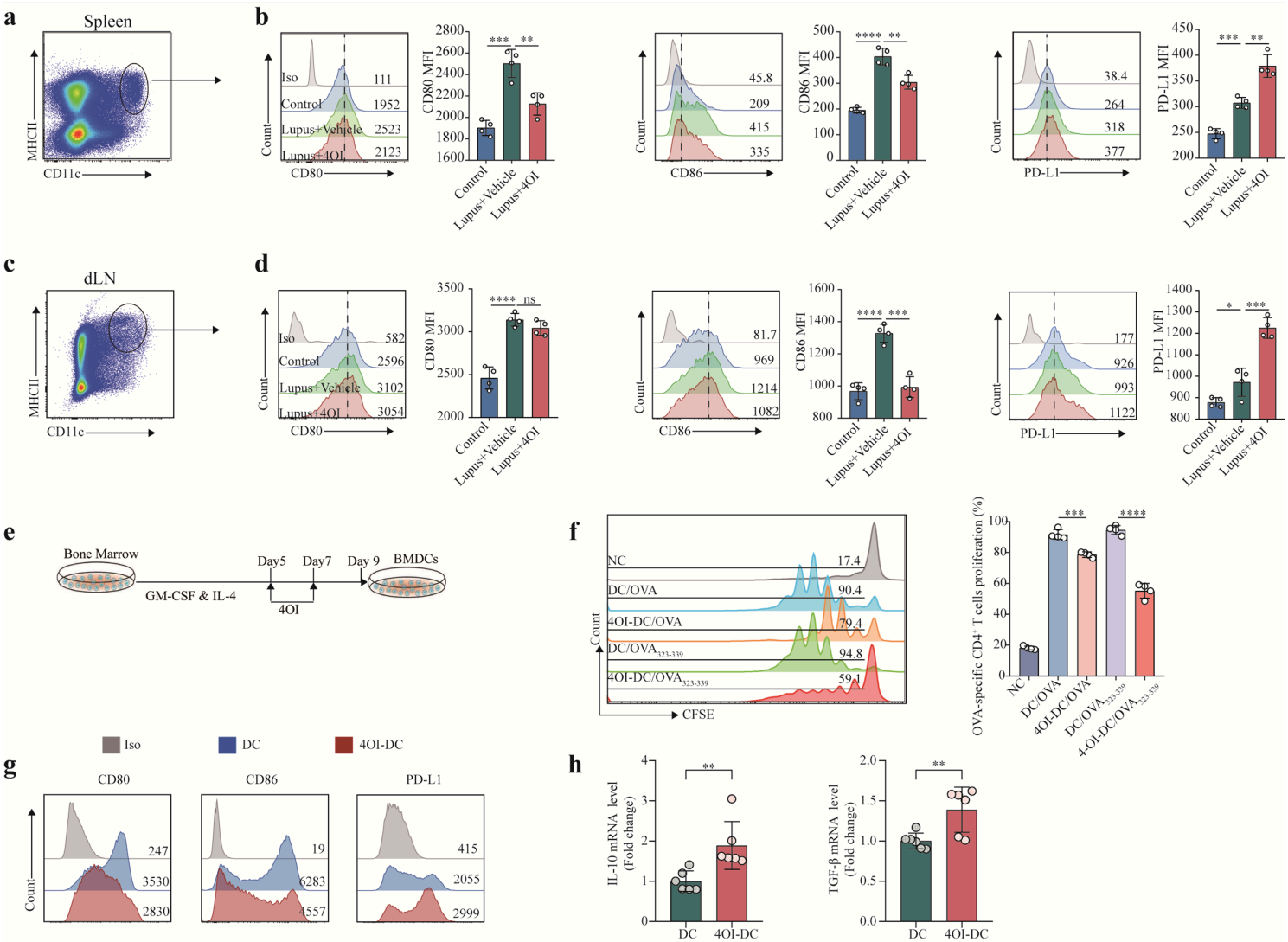


Figure 2

4OI drives the differentiation of tolDCs with tolerogenic phenotype in vivo and in vitro. (a-d) From the first day of the third week of the first immunization, chromatin-induced lupus mice were intraperitoneally

injected with 4OI or Vehicle (10%DMSO) for four weeks. Mice were sacrificed on week 8 (n = 4 per group). Representative flow cytometry plots of splenic DCs from lupus mice (a). Expression level of CD80, CD86, and PD-L1 in splenic DCs from lupus mice (b). Representative flow cytometry plots of DCs isolated from the draining lymph nodes of lupus mice (c). Expression level of CD80, CD86, and PD-L1 on draining lymph node DCs from lupus mice were analyzed by flow cytometry (d). (e) A schematic diagram showing that 4OI drives BMDCs differentiation toward tolDCs. BMDCs were generated from bone marrow of 8-week-old C57BL/6 mice in GM-CSF and IL-4. 4OI (250μM) was added on days 5 and 7, controls received vehicle. Harvest occurred on day 9. Half-media changes with induction medium containing GM-CSF (20 ng/mL) and IL-4 (5 ng/mL) were performed on days 3, 5, and 7. (f) $CD4^+$ T cells were isolated from the spleen of OT-Ⅱ mice. 4OI-BMDCs/BMDCs were pulsed with OVA (50μg/mL) or OVA peptide ($OVA_{323-339}$, 5μg/mL) for 5 hours, and then 4OI-BMDCs/BMDCs were coculture with purified CFSE-labeled $CD4^+$ OT-II cells for 72 hours. OVA-specific $CD4^+$ T cell assay of proliferation was analyzed by flow cytometry. (g) Expression level of CD80, CD86, and PD-L1 on 4OI-BMDCs/BMDCs were analyzed by flow cytometry. (h) The mRNA expression of IL-10 and TGF-β in 4OI-BMDCs/BMDCs was measured by RT-qPCR analysis. The data were obtained from at least three independent experiments. (means ± SDs; **** $p < 0.0001$; *** $p < 0.001$; ** $p < 0.01$; * $p < 0.05$; ns, no significant.)

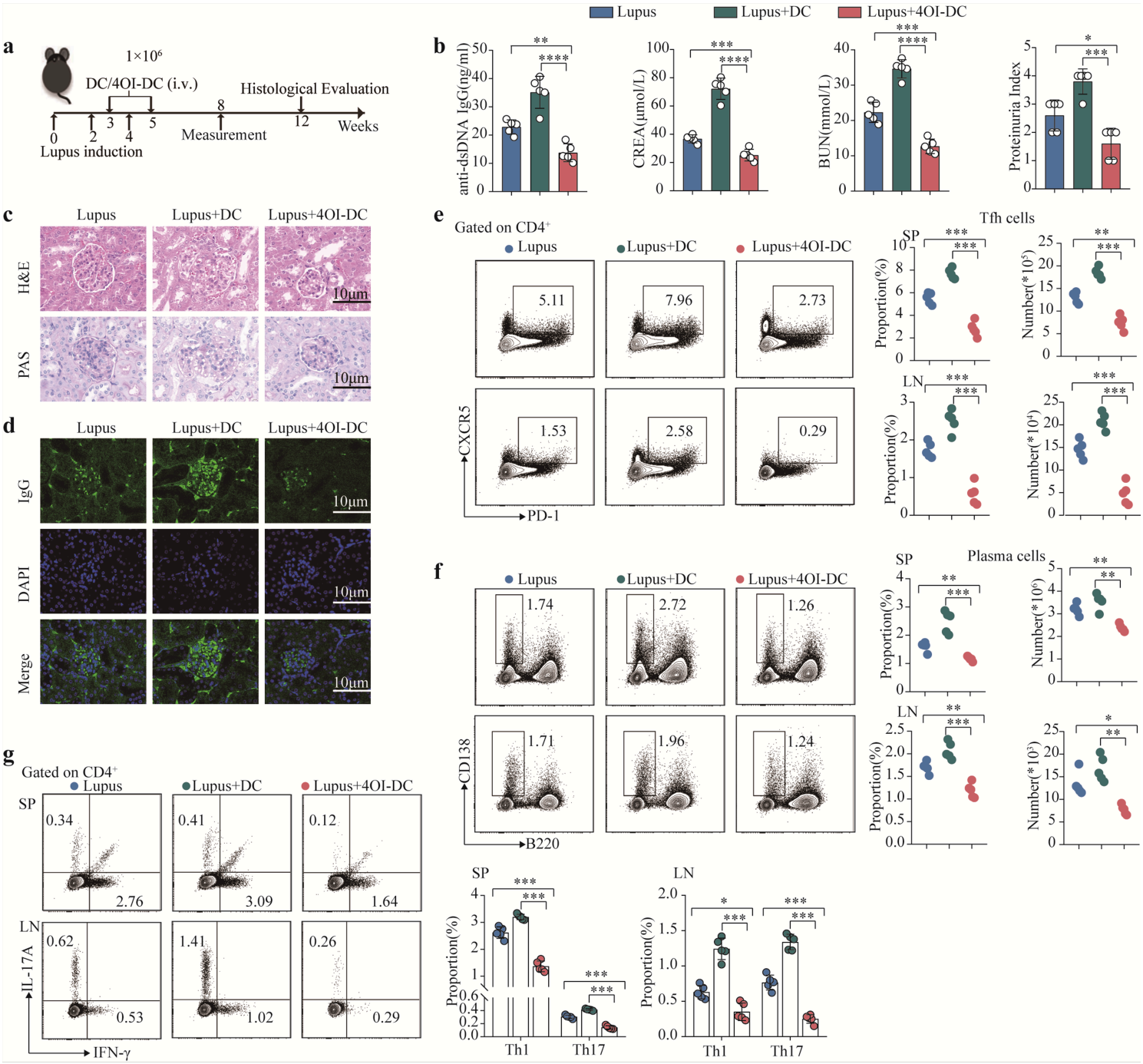


Figure 3

4OI-induced tolDCs attenuates lupus progression. (a-g) Graphic scheme of lupus induction and 4OI-BMDCs administration (a). Eight-week-old female C57BL/6 mice were immunized subcutaneously with chromatin/CFA on week 0, and mice were boosted with chromatin/IFA on weeks 2 and 4. Treatment groups were intravenously injected with 1×10^6 BMDCs/4OI-BMDCs on weeks 3 and 5. Mice were sacrificed on weeks 8 or 12 (n=5 per group). Concentrations of serum anti-dsDNA IgG, creatinine, urea and proteinuria were measured in each group on weeks 8 (b). The histological evaluation of kidney sections in each group was performed with H&E, PAS staining (c), and IgG immunofluorescence staining (d) 12 weeks post first immunization. Scale bar =10μm. Representative flow cytometric profiles and data

plots show the frequencies and numbers of CD4$^+$ CXCR5$^+$ PD-1$^+$ Tfh cells (e), plasma cells (f), CD4$^+$ IL-17A$^+$ Th17 and CD4$^+$ IFN-γ$^+$ Th1 (g) in SP, LNs from each group. The data were obtained from at least three independent experiments. (means ± SDs; **** $p < 0.0001$; *** $p < 0.001$; ** $p < 0.01$; * $p < 0.05$.)

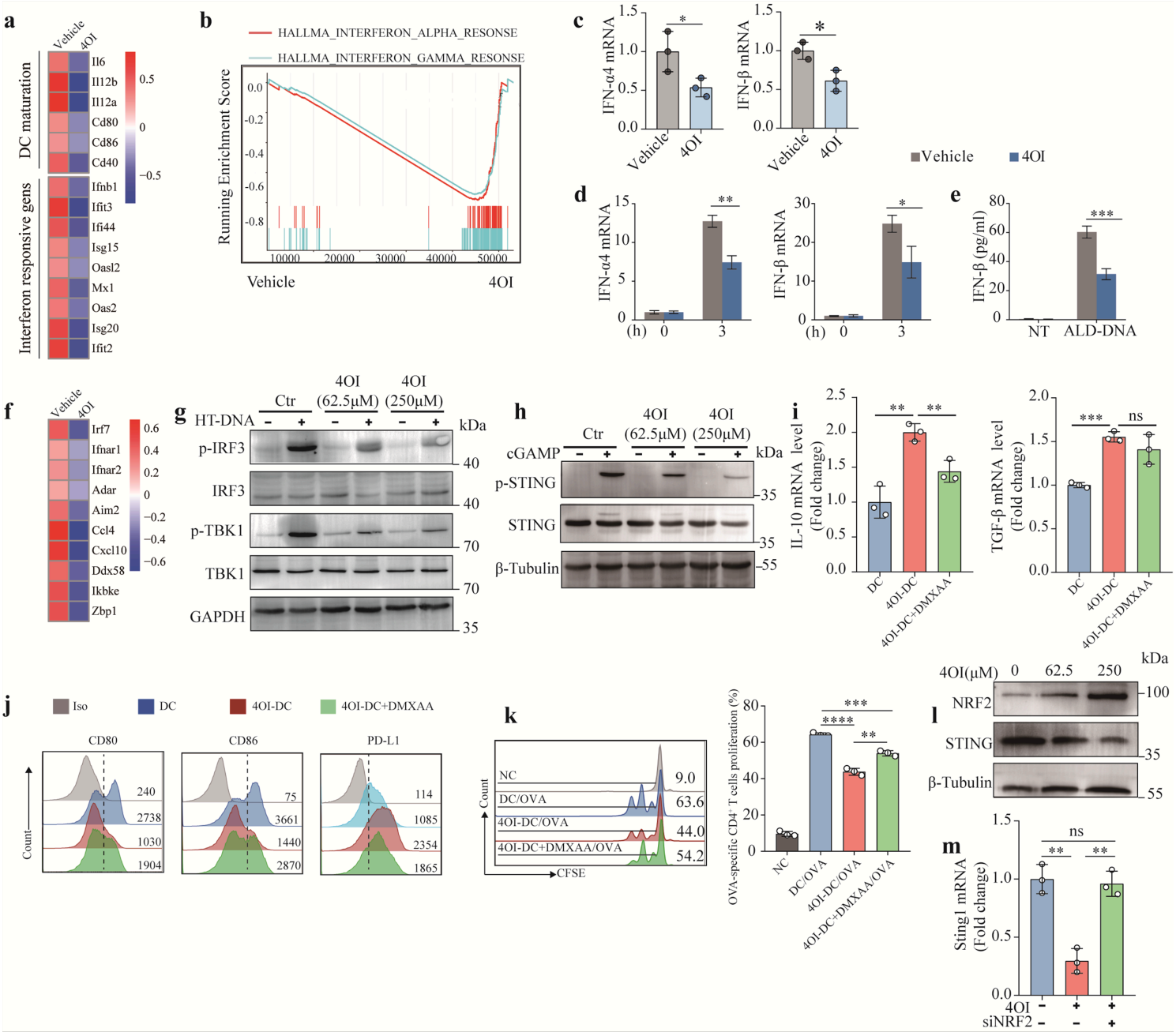


Figure 4

4OI induces DCs tolerance via inhibition of STING transcription and phosphorylation. (a) RNA sequencing analysis using the CD11c$^+$ DCs isolated from the spleen of 4OI-treated and control lupus mice, showing a heatmap of IFN-responsive genes and genes associated with DC maturation. (b) GSEA of the signature genes involved in the type Ⅰ IFN response signaling in the CD11c$^+$ DCs isolated from the spleen of 4OI-treated and control lupus mice. (c) qRT-PCR analysis of the indicated genes in the isolated CD11c$^+$ DCs from the spleen of 4OI-treated and control lupus mice. (d-e) The relative mRNA amount and

protein concentration of 4OI-BMDCs/BMDCs stimulated with 10μg/mL ALD-DNA for the indicated time (d) or 24 h (e) were determined by qRT-PCR and ELISA. NT, non-treated. (f) A heatmap of downregulated genes associated with cytosolic DNA sensing pathway in $CD11c^+$ DCs isolated from the spleen of 4OI-treated relative to control lupus mice. (g) Immunoblot analysis of indicated protein in whole-cell lysates of 4OI-BMDCs/BMDCs stimulated with 10μg/mL HT-DNA for 3h. (h) Immunoblot analysis of indicated protein in whole-cell lysates of 4OI-BMDCs/BMDCs stimulated with 5μg/mL cGAMP for 3h. (i) The mRNA expression of IL-10 and TGF-β in indicated BMDCs was measured by RT-qPCR analysis. (j) Expression level of CD80, CD86, and PD-L1 on indicated BMDCs were analyzed by flow cytometry. (k) BMDCs were coculture with purified CFSE-labeled $CD4^+$ OT-II cells for 72 hours. OVA-specific $CD4^+$ T cell assay of proliferation was analyzed by flow cytometry. (l) Immunoblot analysis of indicated protein in whole-cell lysates of 4OI-BMDCs/BMDCs. (m) qRT-PCR analysis of the Sting1 in the indicated BMDCs. The data were obtained from at least three independent experiments. (means ± SDs; **** $p < 0.0001$; *** $p < 0.001$; ** $p < 0.01$; * $p < 0.05$; ns, no significant).

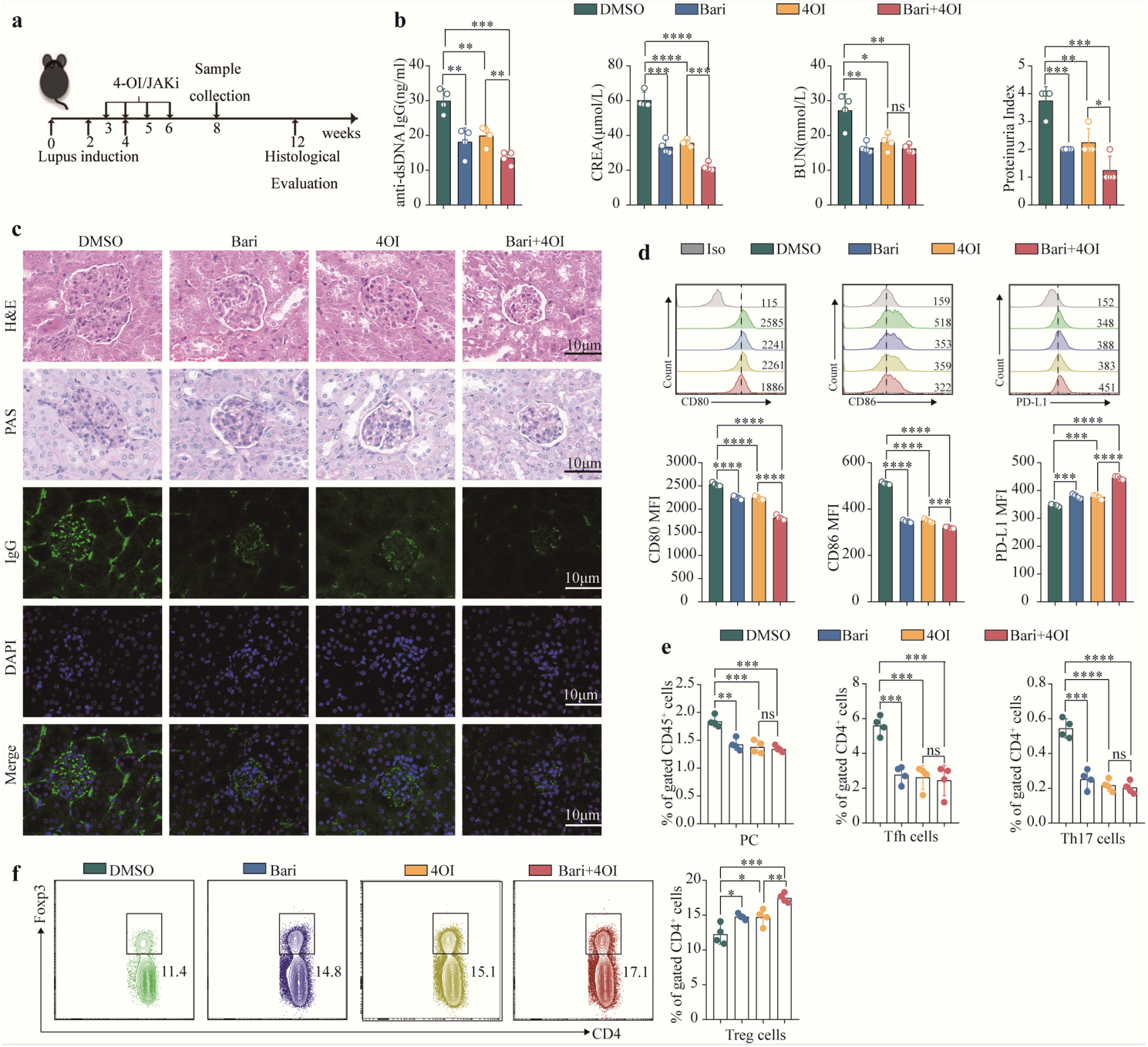


Figure 5

4OI synergize with JAK inhibitor in the treatment of Lupus. (a) Schematic of the kinetic animal experiments in which lupus mice were treated with 4OI (25mg/kg) or JAK inhibitor baricitinib (5mg/kg) alone or in combination (n=4 per group). (b) Concentrations of serum anti-dsDNA IgG, creatinine, urea and proteinuria were measured in each group on weeks 8. (c) The histological evaluation of kidney sections in each group was performed with H&E, PAS staining, and IgG immunofluorescence staining 12 weeks post first immunization. Scale bar =10μm. (d)Expression level of CD80, CD86, and PD-L1 on splenic DCs from lupus mice were analyzed by flow cytometry. (e) The frequencies of plasma cells, $CD4^+$ $CXCR5^+$ $PD\text{-}1^+$ Tfh cells, and $CD4^+$ $IL\text{-}17A^+$ Th17 in SP from each group. (f) Representative flow cytometric profiles and data plots show the frequencies of Treg cells in SP from each group. The data

were obtained from at least two independent experiments. (means ± SD; **** $p < 0.0001$; *** $p < 0.001$; ** $p < 0.01$; * $p < 0.05$; ns, no significant).

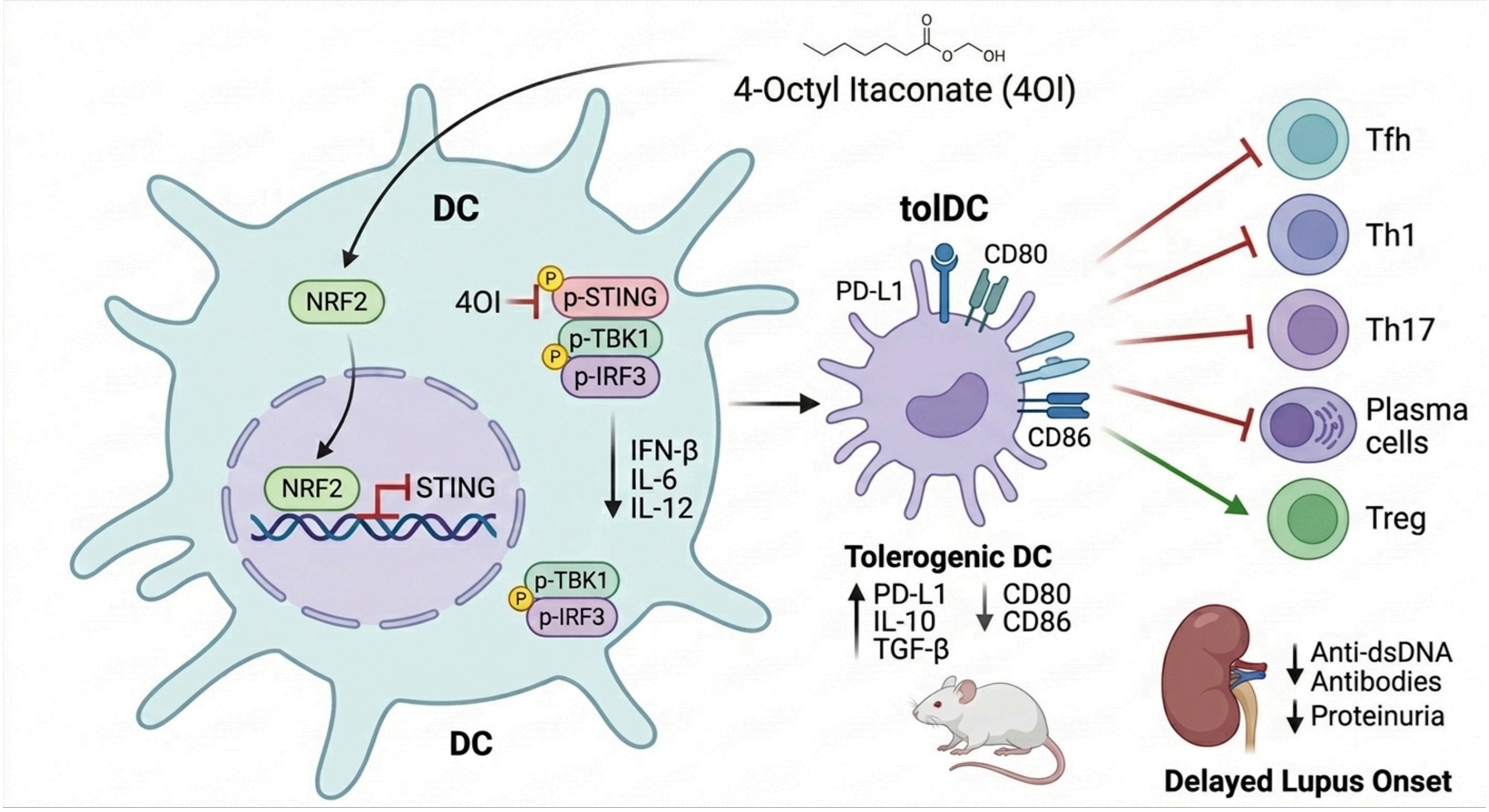


Figure 6

Schematic demonstrating that 4OI-induced tolDCs delay lupus onset in mice. 4OI acts via two distinct, parallel molecular mechanisms: it activates NRF2 to repress STING transcription, and it directly inhibits STING phosphorylation, thereby robustly dampening downstream STING signaling. This concerted dual blockade instructs the differentiation of DCs toward a tolerogenic phenotype(tolDCs). These tolDCs efficiently suppress autoreactive Th1, Th17, and Tfh-cell responses, as well as the differentiation of pathogenic plasma cells. Conversely, 4OI-induced tolDCs effectively promote the expanded generation of Treg cells, thereby potently delaying the development of lupus-like autoimmunity in mice. Image generated with the assistance of Nano Banana Pro.

Supplementary Files

This is a list of supplementary files associated with this preprint. Click to download.

- SupplementaryMaterials.docx